

THE ACS VIRGO CLUSTER SURVEY. XVII. THE SPATIAL ALIGNMENT OF GLOBULAR CLUSTER SYSTEMS WITH EARLY-TYPE HOST GALAXIES*

QIUSHI WANG^{1,2}, ERIC W. PENG^{1,3,4}, JOHN P. BLAKESLEE⁵, PATRICK CÔTÉ⁵, LAURA FERRARESE⁵, ANDRÉS JORDÁN⁶, SIMONA MEI^{7,8}, AND MICHAEL J. WEST^{9,10}

Accepted for publication in The Astrophysical Journal

ABSTRACT

We study the azimuthal distribution of globular clusters (GCs) in early-type galaxies and compare them to their host galaxies using data from the ACS Virgo Cluster Survey. We find that in host galaxies with visible elongation ($\epsilon > 0.2$) and intermediate to high luminosities ($M_z < -19$), the GCs are preferentially aligned along the major axis of the stellar light. The red (metal-rich) GC subpopulations show strong alignment with the major axis of the host galaxy, which supports the notion that these GCs are associated with metal-rich field stars. The metal-rich GCs in lenticular galaxies show signs of being more strongly associated with disks rather than bulges. Surprisingly, we find that the blue (metal-poor) GCs can also show the same correlation. If the metal-poor GCs are part of the early formation of the halo and built up through mergers, then our results support a picture where halo formation and merging occur anisotropically, and where the present day major axis is an indicator of the preferred merging axis.

Subject headings: galaxies: elliptical and lenticular, cD — galaxies: dwarf — galaxies: evolution — galaxies: star clusters : general – globular clusters: general

1. INTRODUCTION

The classical illustration of a globular cluster system is as a spherical halo population around the host galaxy. Galaxies themselves, however, can have a wide variety of shapes, from nearly-spherical to highly anisotropic. There are many reasons why GC systems and stellar halos could be spherical. They could have formed very early in a chaotic fashion, similar to the classic “monolithic collapse”, before dissipation could collect gas into a disk. They could also have originally formed in disks but then had their orbits distributed into a spherical halo via major mergers (e.g., Toomre & Toomre 1972). It is also possible that at least some halo stars and GCs have been accreted from a more spherically distributed population of dwarf-like galaxies and halos (e.g., Searle & Zinn 1978; Côté, Marzke, & West 1998).

It is not necessary, however, that in all cases the shape

of the stellar halo and its GC system be decoupled from its host. Mergers along a preferred axis in a galaxy cluster can produce alignment between the major axis of the brightest cluster galaxy (BCG) and the cluster major axis, as can intrinsic elongation of the dark matter halo (Binggeli 1982; West 1994; Hashimoto, Henry & Boehringer 2008). The distribution of satellites is also not necessarily isotropic around galaxies, as alignments between satellites and host galaxies have been found in many studies, although not always in the same sense. Holmberg (1969) and others (e.g., Zaritsky et al. 1997) found that satellites of disk galaxies tend to be close to the minor axes of their hosts, but other studies (e.g., Brainerd 2005; Yang et al. 2006; Bailin et al. 2008) have found that satellites are preferentially along the major axes of galaxies, particularly early-types.

The oldest stars in the Universe are found in stellar halos and GCs, and these populations are the oldest visible collisionless tracers within galaxies. The shapes of halo stellar populations tells us about the merging and accretion history of the galaxy over a Hubble time. Studying the outer shapes of stellar halos, however, is extremely difficult because of their low surface brightnesses. Globular clusters, however, are readily identified out to large distances using the Hubble Space Telescope ($D \lesssim 100$ Mpc, e.g., Peng et al. 2011), and are present in nearly every galaxy except the faintest dwarf galaxies. GC systems in massive galaxies are also known to have bimodal color distributions, which may correspond to “metallicity subpopulations” whose mean metallicities correlates with the mass of the host galaxy (e.g., Larsen et al. 2001; Peng et al. 2006a). Although the exact interpretation of these color distributions in metallicity is currently debated (c.f., Yoon et al. 2006, 2011), it is still true that with reasonably deep imaging, GCs can be easily detected, and can provide some chemical information on the underlying stellar population.

Recent studies of extragalactic GC systems have taken

* Based on observations with the NASA/ESA *Hubble Space Telescope* obtained at the Space Telescope Science Institute, which is operated by the Association of Universities for Research in Astronomy, Inc., under NASA contract NAS 5-26555.

¹ Department of Astronomy, Peking University, Beijing 100871, China

² Physics Department, New York University, 4 Washington Place, New York, NY 10003, USA

³ Kavli Institute for Astronomy and Astrophysics, Peking University, Beijing 100871, China

⁴ Corresponding author; peng@pku.edu.cn

⁵ Herzberg Institute of Astrophysics, National Research Council of Canada, 5071 West Saanich Road, Victoria, BC V9E 2E7, Canada

⁶ Departamento de Astronomía y Astrofísica, Pontificia Universidad Católica de Chile, Casilla 306, Santiago 22, Chile

⁷ University of Paris 7 Denis Diderot, 75205 Paris Cedex 13, France

⁸ GEPI, Observatoire de Paris, Section de Meudon, 5 Place J. Janssen, 92195 Meudon Cedex, France

⁹ Maria Mitchell Observatory, 4 Vestal Street, Nantucket, MA 02554, USA

¹⁰ European Southern Observatory, Alonso de Cordova 3107, Vitacura, Santiago, Chile

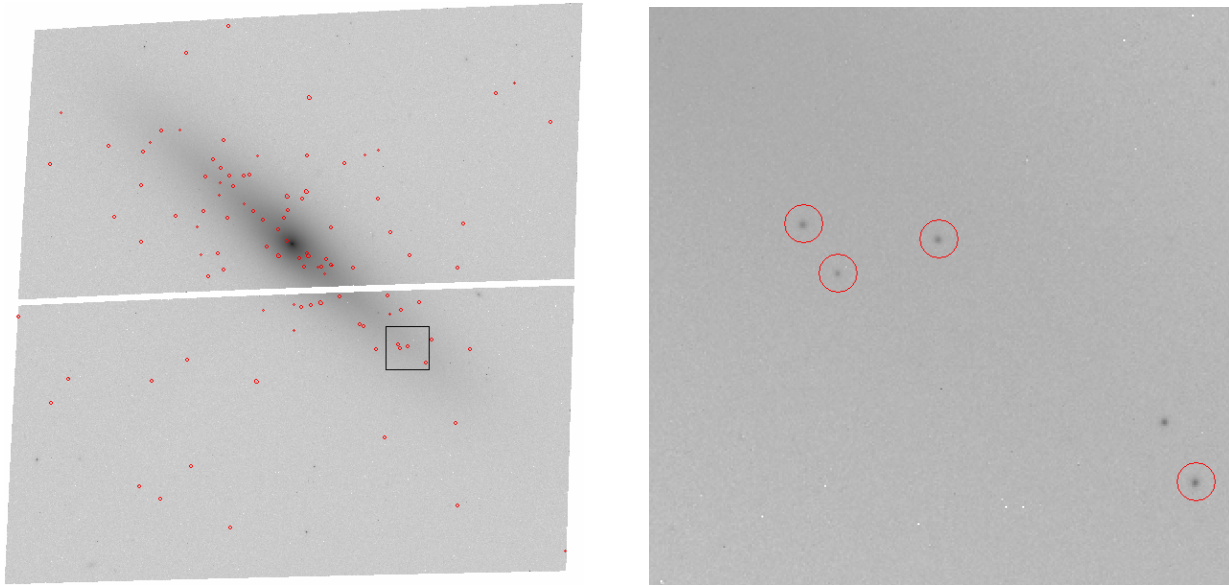


FIG. 1.— Left panel: VCC 1692 and globular cluster candidates with $class > 0.9$. The white gap in the middle of the image is the gap between two WFC detectors. Right panel: enlarged image of the squared area in the left.

advantage of surveys of early-type galaxies using *HST*, particularly in the Virgo and Fornax galaxy clusters. In this paper, we undertake a study of the azimuthal distributions of GC systems in early-type galaxies using data from the ACS Virgo Cluster Survey (Côté et al. 2004). The high spatial resolution and depth of this survey has already been used to study GC color distributions (Peng et al. 2006a), size distributions (Jordán et al. 2005), luminosity functions (Jordán et al. 2006, 2007), formation efficiencies (Peng et al. 2008), and color-magnitude relations (Mieske et al. 2006, 2010), as well as other dense stellar systems such as diffuse star clusters (Peng et al. 2006b), ultra-compact dwarfs (Hasegan et al. 2005) and nuclear star clusters (Côté et al. 2006; Côté et al. 2007). This data set is well-suited to the study of star clusters in Virgo early-type galaxies, and we use the GC catalog of Jordán et al. (2009).

In this paper, we seek to answer the questions: 1) Can GC systems be non-spherical? 2) If so, does the major axis of the GC system have any relationship with that of the host galaxy? 3) Do the blue and red GC subpopulations have different distributions around their hosts? The GC systems of a few massive galaxies have been shown to be flattened (e.g. McLaughlin et al. 1994, 1995), but in this paper, we present the first large study of GC systems and their possible alignment with their host galaxies.

2. DATA AND METHODS

2.1. Globular Cluster Catalog

The ACS Virgo Cluster Survey (ACSVCS; Côté et al. 2004) observed one hundred Virgo Cluster early-type galaxies in two filters F475W (g) and F850LP (z). We use the globular cluster catalog for all ACSVCS galaxies presented by Jordán et al. (2009), which gives their positions, photometry, half-light radii, and a $class$ parameter which indicates the probability a given object is a GC (see Jordán et al. 2004 for the specifics of the data reduction). By the virtue of the high resolution of Hubble Space Telescope (*HST*), we can measure the total magnitude z_0 and half light radius r_h of every globular

cluster candidate. The GC probability is determined using these parameters in comparison to control fields customized for the observational depth for each galaxy (see Peng et al. 2006a, Figure 1). In this paper, we select objects with $class > 0.9$ as GCs. This is more similar to the stringent selection used in the GC system color gradient study of Liu et al. (2011), which also required strict selection against background contaminants. For the dwarf galaxies in the sample (where contamination is highest and potentially a larger issue), we estimate from control fields that there should be only ~ 1.5 contaminants per galaxy selected by our size-magnitude-color criteria. This extremely low level of contamination minimizes the effect of anisotropy in the background.

This selection does not include the objects discussed as “faint fuzzies” in Larsen & Brodie (2000) or “diffuse star clusters” (DSCs) in Peng et al. (2006b). In cases where a distance is needed, we use the SBF distances presented in Blakeslee (2009, also see Mei et al. 2007). We use a mean distance of 16.5 Mpc to the Virgo Cluster (Mei et al. 2005).

Several galaxies in the ACSVCS sample are in close proximity to large neighboring galaxies, and their GC systems are either overwhelmed by the GC system of their neighbor, or strongly depleted in GCs, possibly due to tidal stripping. We exclude these six galaxies from our analysis: VCC 1327, VCC 1297, VCC 1279, VCC 1938, VCC 1192 and VCC 1199.

2.2. Methodology

The relatively wide field of view of the ACS/WFC ($202'' \times 202''$, or 16.2×16.2 kpc), allows us to study the azimuthal distribution of GC systems in all but a few of the more massive galaxies in the ACSVCS sample. The image of one ACSVCS galaxy, VCC 1692, is shown in Figure 1. This lenticular galaxy is the twelfth brightest galaxy in the ACSVCS sample, and provides a nice example to illustrate our analysis methods. As can be seen even by eye, the globular clusters in VCC 1692 tend to align with the galaxy light, and are preferentially

clustered close to the plane of the galaxy (Figure 1, left). Our goal is to quantify this, particularly in galaxies where the geometry may not be so favorable.

To do this, we analyze the distribution of GCs in azimuth (position angle, ϕ). This approach, rather than a more complicated fitting of isopleths, is applicable to a wide range of data, from the relative large GC system shown in Figure 1 to the smaller ones belonging to dwarf galaxies. We use the azimuthal distribution to test for departures from circular symmetry. In cases where the azimuthal distribution appears anisotropic, we can also test for alignment between the major axis of the GC system and that of the galaxy.

This test, looking for departures from uniformity in the projected azimuthal distribution, is in many ways the simplest one we can do. Understanding the intrinsic shapes of GC system is a much more difficult question that would require incorporating inclination, not to mention many more intrinsic parameters. This paper is a simple, but interesting first step to generally study anisotropic spatial distributions in GC systems.

We analyze the azimuthal distributions of GCs using two methods. First, we use the Kolmogorov-Smirnov (K-S) test to test for departures from a random (isotropic) distribution. Second, we use binned distributions in azimuth to see if the GC system has a preferred axis.

2.3. Generating Random Comparison Samples

To perform these tests, we need to create control samples that mimic a random azimuthal distribution of GCs (the equivalent to an isotropic, or spherical, GC system). Because the boundary of the image is not a circle, and the center of the galaxy is not exactly at the position of the image center, the observed area in a given $\Delta\phi$ changes with azimuth (ϕ). Therefore, an azimuthally random distribution of GCs about the galaxy will not result in a constant observed number per unit azimuth. Taking a mean surface number density as a function of ϕ is also problematic because this density changes as function of projected radius from the galaxy center.

For each galaxy, we create a “randomized” sample of GCs purely in azimuth, bypassing the need to know the radial density profile of the GC system. For each GC, we first assign it a random angle position while keeping its projected radius unchanged. We then see if the randomized position is within the image area of the galaxy. If not, we randomize it again as in the first step, until the resulting globular cluster is located within the image. We continue to do this for each GC in the sample until all GCs have new positions within the observed area of the image, creating a fully randomized control sample. By “randomized”, we mean that the GCs in the image randomly populate the distribution in azimuth, modulo the varying image area, and without needing to make assumptions about the GC radial density profile. We define N as the number of control samples we generate. Unless mentioned otherwise, N in our study equals one thousand.

Some of the objects classified as GCs will in fact be contamination from background galaxies. Assuming that background objects are distributed isotropically in azimuth, their only effect is to dilute the signal of any alignment within the GC system. Including them in the randomized samples should not introduce a bias unless

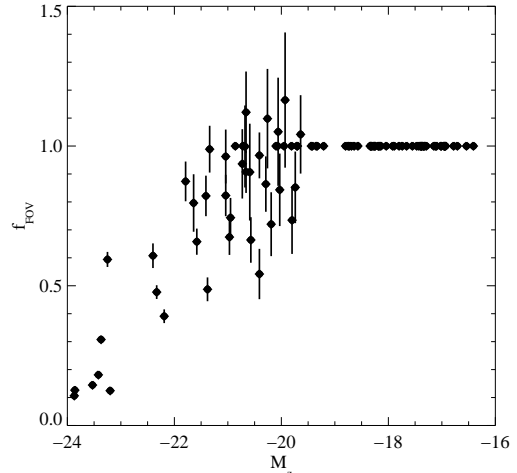


FIG. 2.— For the more luminous galaxies in our sample, the ACS/WFC field of view covers only a fraction of the full GC system. We plot this fraction against M_z to show that for systems with $M_z \lesssim -20$ mag, we are missing a measureable fraction of GCs. Galaxies for which the ratio is exactly unity are those for which ACS/WFC field is presumed to cover the entire GC system. Values larger than unity are due to errors in fitting the total number of GCs from the GC radial density profile. Only 9 of the 94 galaxies in the sample have less than 50% coverage.

they are not isotropically distributed in the field of view. Fortunately, the GC samples are already quite clean of contaminants, with an expectation of only ~ 1.5 background objects per galaxy (Liu et al. 2011).

We also analyze the azimuthal distributions of the GC color subpopulations. We divide the GCs into blue and red populations using their $(g-z)$ color. For the more massive GC systems, we use the two-Gaussian mixture model fits from Peng et al. (2006a) to determine the crossover color between the two populations. For galaxies where there are fewer GCs, we choose a color of $(g-z) = 1.10$ mag to separate blue from red. We ultimately performed all of our analysis using a stricter separation between the two populations ($(g-z) < 1.00$ for blue GCs and $(g-z) > 1.20$ for red GCs. None of our conclusions change when we change the color cuts. When analyzing the color subpopulations, we generate separate randomized samples for each one.

2.4. The HST/ACS Field of View

One of the main limitations of our study is the ACS/WFC field of view. This characteristic of the ACSVCS sample has been described in previous studies (particularly in Peng et al. 2008, Section 3), but we further quantify the issue in this paper. For most of the early-type dwarf galaxies in the sample, the $202'' \times 202''$ ACS field of view is more than adequate to cover the entire GC system, but this is not the case for galaxies with $M_z \lesssim -20$ mag. We illustrate this in Figure 2, where we show the fraction of the entire GC system included in the ACS/WFC field of view. This total number of GCs for larger GC systems was determined using a Sérsic fit to the spatial density profile (Peng et al. 2008). Where the ratio is exactly unity (for most dwarfs), the total number was determined to be the number observed in the ACS/WFC field. For the most luminous galaxies in our sample, only $\sim 10\%$ of the GCs are being analyzed. Nevertheless, the quality of the data is high and

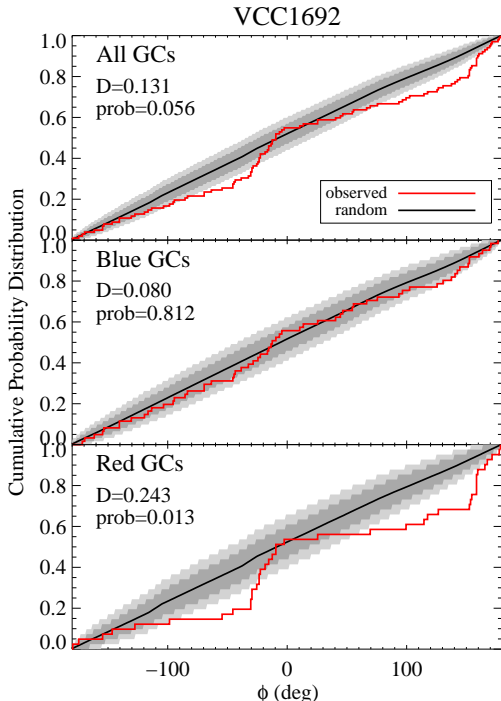


FIG. 3.— VCC1692. The top, middle and bottom plots show the cumulative probability distributions (CPDs) of GCs versus position angle (degrees east from north) for all, blue and red GCs, respectively. The red lines represent the observed distribution, and the black lines represent the sum of 10000 randomized samples. The dark gray and light gray regions are the regions encompassing 68% and 90%, respectively, of all randomly generated samples. The values for the D statistic and the probability that the two samples were drawn from the same distribution are labeled in each plot. Note the large excesses above the random distribution at -35° and $+145^\circ$. These correspond to GCs preferentially clustered around the galaxy major axis. The effect is more pronounced for the red GCs.

we can still draw interesting conclusions from these inner regions. Most of our sample, however, is not particularly compromised; in only nine of our 94 galaxies do we sample less than half of the GC system. Similar analyses of the full GCS at large radii will require wide-field imaging, like those in the Next Generation Virgo Survey (Ferrarese et al. 2012).

3. RESULTS

3.1. The Kolmogorov-Smirnov Test

We employ the two-sided Kolmogorov-Smirnov test to quantitatively study the alignment between GC systems and their host galaxies. Specifically, for each galaxy, first we create randomized samples as described above, then we use the Kolmogorov-Smirnov test to compare the randomized distribution with the observed one. The result can be displayed visually in the cumulative distributions of both observed and randomized samples. These distributions for the galaxy VCC1692 are shown in figure 3. There are two evident knee-like steps in the red GCs' cumulative azimuthal distribution, spaced 180° apart, which indicates an alignment along an axis. The cumulative distribution of the blue GCs also show these two steps, but to a lesser degree.

The two-sided K-S test generates the D statistic, which is a measure of the maximum deviation of one cumula-

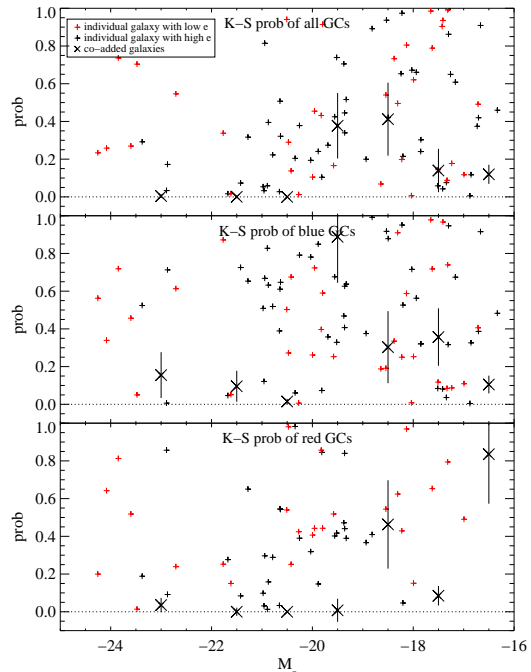


FIG. 4.— K-S test results for individual galaxies and binned galaxy samples. These figures plot the probability that the azimuthal distribution of GCs is drawn from a random distribution ($prob$) against the total luminosity of the galaxy. Results are plotted for all GCs (top), blue GCs (middle), and red GCs (bottom). Small red points are galaxies with ellipticities, e , less than 0.2. Small black points are galaxies with ellipticities, e , greater than 0.2. Large points with error bars represent galaxies binned samples of galaxies with $e > 0.2$. For all samples of GCs, the more luminous galaxies, on average, have anisotropic GC systems.

tive probability distribution from another. This statistic results in a probability that the two data sets are drawn from the same distribution. We have calculated the distribution of D statistic values using our observed data and each of the 10000 azimuthally randomized samples. We find that this distribution is well-behaved and nearly Gaussian. In the case of VCC 1692, there is only a 5.6% probability that its GCs are drawn from a random azimuthal distribution. The probability is even lower, 1.3% for the red GCs alone. The distribution of blue GCs is much closer to that of the randomized sample, with a 81.2% of being drawn from a random distribution.

In Figure 4, we plot the results of the K-S test for all galaxies in the sample. For each galaxy, we plot $prob$, $prob_{blue}$, and $prob_{red}$, which are the probabilities that the entire GC system, the blue GCs, and the red GCs are drawn from a random distribution, respectively. We plot these probabilities as a function of the absolute z magnitude of the galaxy (M_z). The galaxy magnitudes are from Ferrarese et al. (2006) and Peng et al. (2008).

Figure 4 shows that there is a large scatter in probabilities for the ACSVCS galaxies. The brightest galaxies suffer from a small field of view, and the less luminous galaxies have few GCs, creating increased scatter. For some galaxies, however, particularly those with $-23 < z < -21$ mag, the probability that the GCs are distributed in random azimuth is very small. These galaxies tend to be lenticular or elliptical galaxies with high axis ratio. To highlight this, we plot with differ-

TABLE 1
KOLMOGOROV-SMIRNOV PROBABILITIES FOR BINNED GALAXIES
SAMPLES.

M_z range	$prob_{\text{all}}$	$prob_{\text{blue}}$	$prob_{\text{red}}$
-24, -22	0.004±0.010	0.155±0.122	0.035±0.038
-22, -21	0.000±0.008	0.096±0.082	0.000±0.022
-21, -20	0.000±0.000	0.015±0.014	0.000±0.000
-20, -19	0.377±0.173	0.888±0.244	0.008±0.061
-19, -18	0.412±0.193	0.303±0.191	0.463±0.234
-18, -17	0.140±0.115	0.357±0.152	0.085±0.052
-17, -16	0.120±0.051	0.105±0.047	0.836±0.263

Note - $prob_{\text{all}}$, $prob_{\text{blue}}$ and $prob_{\text{red}}$ are the probabilities that the azimuthal distribution of GCs is drawn from a random distribution, for all, blue and red GCs, respectively. The uncertainty is obtained by bootstrap. Only galaxies with ellipticities greater than 0.2 are included in the bins

ent colors the galaxies with ellipticities $\epsilon > 0.2$, which are taken from the isophotal fitting of Ferrarese et al. (2006, see their Figure 121 for the relationship between ellipticity and luminosity).

Since some galaxies are so faint that there are too few detected globular clusters to determine the trends, we bin galaxies by their magnitudes and run the Kolmogorov-Smirnov test on the collective data sets. If GC systems are possibly aligned with the shapes of their host galaxies, then non-spherical galaxies provide a stronger test of this hypothesis, so we only include galaxies with $\epsilon > 0.2$ in the binned samples. When combining galaxies, we always use a GC’s position angle from the galaxy major axis. This should enhance the signal if GC systems are aligned with the galaxy light, but would decrease the signal if GC systems are randomly oriented with respect to their hosts. We use the major axis position angles given by Ferrarese et al. (2006), averaging the values given for the g and z bands.

Furthermore, we use the bootstrap to determine the errors in the probabilities produced by the Kolmogorov-Smirnov test. The results are shown in Table 1. In Figure 4, we plot the result of Kolmogorov-Smirnov test for individual galaxies and binned samples (with error bars). For the binned samples of galaxies with $\epsilon > 0.2$ in particular, we can clearly see the trends of GC systems. The most obviously anisotropic distributions of GCs are for the red GCs in the four most luminous galaxy bins. For this magnitude range ($M_z \lesssim -19$ mag), on average, the probability that the GCs are isotropically distributed in azimuth about the galaxy is near zero. This is also true, however, for the blue GCs in the three most luminous bins ($z \lesssim -20$ mag). Once we get down to dwarf galaxy luminosities, the alignment between the GC systems and the galaxies is less evident. This might be because dwarfs have more spherical systems, or that there are fewer GCs per galaxy so the noise reduces the signal.

3.2. Azimuthal Distribution

In order to further investigate whether the non-random distribution of GCs has something to do with the host galaxy, we plotted the histogram of GCs as a function of the azimuthal angle from the galaxy major axis. We assume that the distribution is axisymmetric in nature, and we define the major axis of the galaxy to be at $\phi' = 0^\circ$, and all GCs to have ϕ' to be within the interval $[-90^\circ, 90^\circ]$. Specifically, if a given GC’s position angle is out of this interval, we add or subtract 180° .

In an axisymmetric system, this arrangement doubles the magnitude of the signal in the peak, if any.

Let us designate the number of observed GCs in a bin by N_{ob} and that of randomized GCs by N_{ran} which is the mean in a bin over the randomized samples. We define the “excess” quantity E as:

$$E = N_{\text{ob}} - N_{\text{ran}} \quad (1)$$

We assume the number of GCs in a bin observes a Poisson distribution, and we can get the estimate of the deviation of E where N is the times we do randomization ($N = 1000$):

$$\sigma = \sqrt{N_{\text{ob}} + \frac{N_{\text{ran}}}{N}} \quad (2)$$

For illustration, we show the azimuthal distribution for VCC 1692 in Figure 5. We find that the red GCs significantly align with the galaxy’s major axis, and the blue GCs also show this trend, but to a lesser extent. For most galaxies, the azimuthal histograms are quite noisy due to the low number of GCs. Therefore, like in the previous section, we determine the azimuthal distributions of the binned galaxy samples. We select our galaxies and combine the GC systems in the same way as we did for the K-S test, as shown in Table 1.

The combined azimuthal GC distributions for the binned samples are plotted in Figures 6 and 7. As with the K-S test, we find that the GC azimuthal distribution is significantly anisotropic for the brighter galaxies. In this case, we establish that the GCs are aligned along the major axis of their hosts. The galaxies that show this trend most strongly are those that have magnitudes in the range $-22 < M_z < -20$, where it is seen unambiguously for both blue and red GCs.

4. DISCUSSION

Our results indicate that for luminous early-type galaxies with moderate to high ellipticity, the spatial distribution of GCs is aligned with the stars in the host galaxies. For galaxies with small ellipticity, the GCs tend to be more randomly distributed, but this neither proves nor disproves the hypothesis that GCs are following the galaxy light. The alignment appears strongest in our data for galaxies around intermediate luminosity ($-22 < M_z < -19$). Early-type galaxies in this luminosity range are preferentially lenticular or more elongated ellipticals. They are also both small enough such that a significant fraction of their GC system is in the ACS/WFC field of view, yet luminous enough to still have substantial GC systems. They are in many ways the best targets for this study, and we see a clear signal for both the red and blue GCs.

The red, metal-rich GCs show the strongest alignment with the major axis of their host galaxies. These GCs are often hypothesized to be formed in same starburst events that formed the bulk of the galaxy (e.g., Ashman & Zepf 1992), so it is unsurprising that they should be closely associated with the bulk of the star light. On the other hand, it is not necessary for them to have been formed together, as metal-rich GCs could have been accreted along the same preferred axis. For lenticular (S0) galaxies that have both bulges and stellar disks, it is interesting to ask whether the red GCs seem to be more associ-

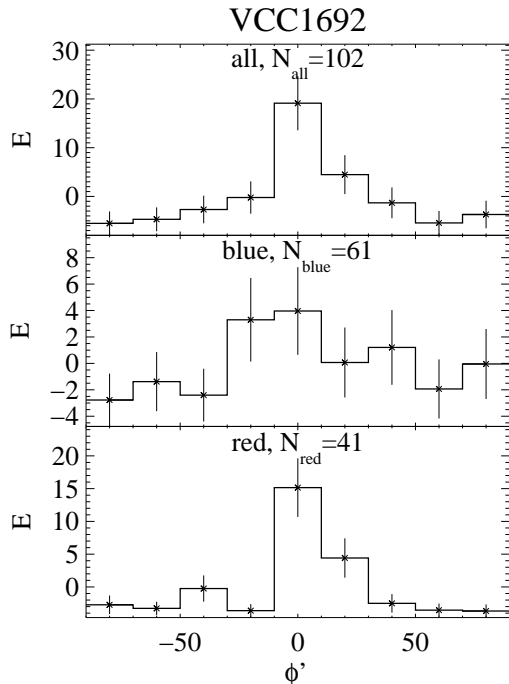


FIG. 5.— VCC1692. The top, middle and bottom plots show the histograms of all, blue, and red GCs, respectively, versus position angle (in degrees, east of north from the major axis). The error bar shows the uncertainty obtained by the equation (2). In all cases, the GC azimuthal distribution shows a strong peak at the position angle of the major axis, showing that the GCs are aligned with the light of their host galaxy.

ated with bulges or disks. In some more edge-on galaxies where we can hope to distinguish disk populations, such as VCC 1692 shown in Figure 1, the GCs do appear to be more disk-like in their distribution. VCC 1062, classified as an SB0, is another example where the red GCs almost exactly trace the disk light. In some early-type galaxies, the metal-rich GCs appear to be more associated with the stellar disk than they are with the bulge.¹

We also find that the blue, metal-poor GCs in the inner regions of luminous early-type galaxies also align with the major axes of their hosts. This result is more surprising, as the canonical metal-poor halo system is usually pictured as spherical. The anisotropy in the distribution of blue GCs is not as pronounced as that for the red GCs, but it is still detected at high significance. This is interesting, as metal-poor GCs often contain some of the oldest stars in the galaxy, and may form in some of the earliest collapsing dark matter overdensities (Moore et al. 2006). Metal-poor halo stars and GCs may also be the best stellar tracer of the overall matter distribution (e.g., Abadi, Navarro, & Steinmetz 2006). That the blue GCs in many of the luminous galaxies appear to have anisotropic azimuthal distributions is a clue that these galaxies did not form their old halos in an environment of isotropic merging, but perhaps were created along local filaments. Brainerd (2005) used the SDSS to find that satellite galaxies within $r_p \lesssim 100$ kpc are also

¹ Previously, Peng et al. (2006b) found that diffuse star clusters in the ACSVCS galaxies tend to be found in lenticular galaxies and were spatially correlated with their disks. The GCs we study in this paper are different from the diffuse star clusters and have magnitudes and sizes typical of GCs.

preferentially aligned along the major axis. If some blue GCs have their origin in merging satellites, then this is a suggestive connection. The connection between satellite dwarfs and halo GCs has been made in kinematic studies (Côté et al. 2001, Woodley 2006), where the rotation axes of metal-poor GCs and satellite dwarfs were found to be aligned. Furthermore, a recent GC kinematic study of M87, the second most luminous galaxy in our sample, indicates that its GC system was possibly affected by a recent merger (Strader et al. 2011; Romanowsky et al. 2012).

The field of view of our data is too small to evaluate the shape of the entire GC system for the luminous galaxies, but it would be very interesting if future wide-field data could extend these studies to larger radii. If metal-poor GCs trace the total mass distribution, then this may give us a visible tracer of the flattening of dark matter halos in these galaxies. Given that these galaxies reside in a dense cluster environment, the shapes of their halos and their GC systems may be unlike that of a galaxy like the Milky Way. The tendency for the more luminous galaxies to show this alignment is similar to the trends seen in the alignment between galaxies their surrounding large scale structure (West & Blakeslee 2000; Wang et al. 2008; Faltenbacher et al. 2009).

The ACS field of view necessarily limits us to studying the “inner halo” populations of the more luminous galaxies. Wide-field imaging, such as that which will be provided by the Next Generation Virgo Cluster Survey (NGVS; Ferrarese et al. 2012), will provide information on the possible alignment of GCs in the outer regions of these galaxies.

5. CONCLUSIONS

We have used data from the ACS Virgo Cluster Survey to study the azimuthal distribution of globular clusters around early-type galaxies. We use the Kolmogorov-Smirnov test in conjunction with tailored control samples to determine the degree of anisotropy in the azimuthal GC distributions of the sample galaxies. We also combine the GC systems of galaxies with similar luminosities. We find that:

- The azimuthal distribution of GCs is strongly anisotropic around early-type galaxies with moderate to high ellipticity ($\epsilon > 0.2$) and intermediate to high luminosity ($M_z < -19$). We see no strong trends for dwarf galaxies.
- In these galaxies, the GCs are preferentially aligned along the major axis of the host galaxy.
- The red GCs exhibit the strongest correlation with galaxy light, and in some cases may be associated with the stellar disks of lenticulars. This association strengthens the idea that the formation of red GCs is linked to that of the metal-rich field star population.
- The blue GCs in these galaxies also show a significant tendency to be aligned with the host galaxy major axis, although to a lesser extent than the red GCs. That the blue GC distributions are also non-spherical in their distribution suggests that these

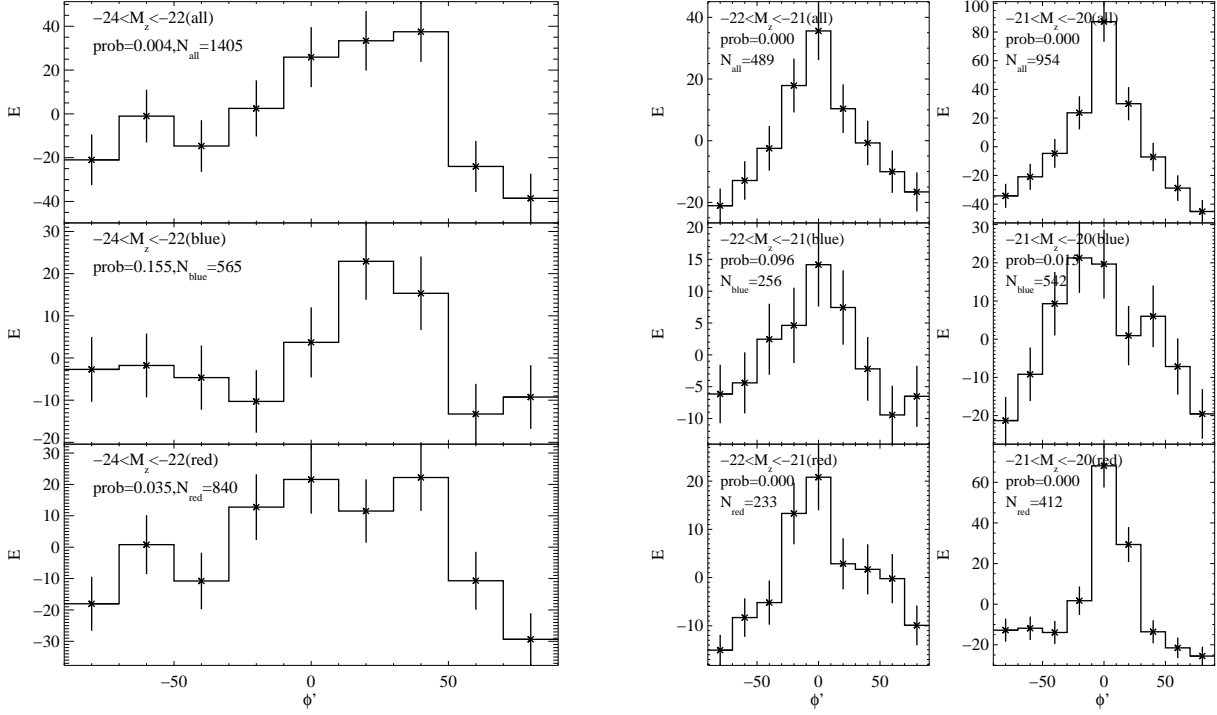


FIG. 6.— Azimuthal distribution of GCs versus position angle (degrees, east of north from the major axis) for samples binned by galaxy luminosity. (Left) All galaxies with $\epsilon > 0.2$ and $-24 < M_z < -22$. (Right) Same as left, but for galaxies with $-22 < M_z < -21$ and $-21 < M_z < -20$. The peak at $\phi' = 0$ deg means that the GCs are clustered around the major axes of their host galaxies. We find this clustering is strong for red GCs, but also very significant for blue GCs. For the more massive bins, the small field of view may dilute the signal.

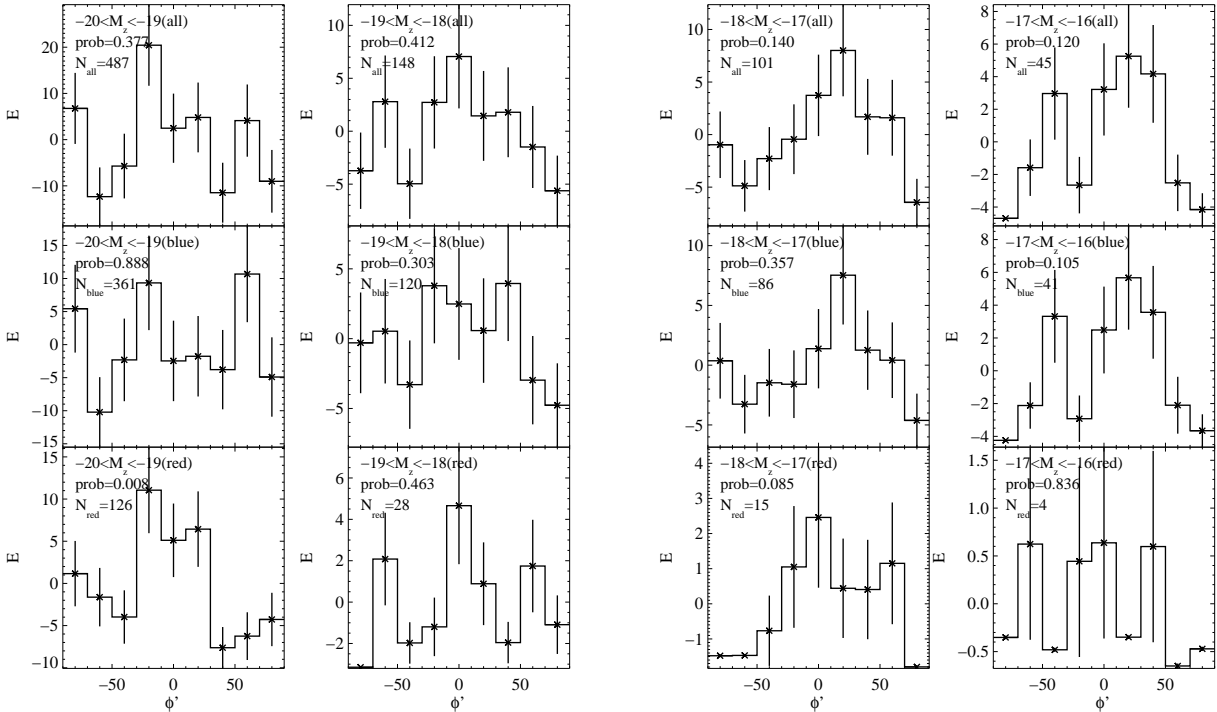


FIG. 7.— Azimuthal distribution of GCs versus position angle (degrees, east of north from the major axis) for samples binned by galaxy luminosity. All galaxies with $\epsilon > 0.2$ and $-20 < M_z < -19$ and $-19 < M_z < -18$ (left), and $-18 < M_z < -17$ and $-17 < M_z < -16$ (right). These binned samples show a strong clustering around the major axes of galaxies, even for dwarfs.

galaxies did not experience mergers from all directions, and instead formed their halos along a direction defined by their current major axis.

E. W. P. gratefully acknowledges support from the Peking University Hundred Talent Fund (985) and grants 10873001 and 11173003 from the National Natural Science Foundation of China. A. J. acknowledges support from BASAL CATA PFB-06 and the Millennium Sci-

ence Initiative, Chilean Ministry of Economy (Nucleus P07-021-F). The authors thank the anonymous referee for comments that improved the paper.

This research has made use of the NASA/IPAC Extragalactic Database (NED) which is operated by the Jet Propulsion Laboratory, California Institute of Technology, under contract with the National Aeronautics and Space Administration.

Facilities: HST(ACS)

REFERENCES

- Ashman, K. M., & Zepf, S. E. 1992, *ApJ*, 384, 50
 Bailin, J., Power, C., Norberg, P., Zaritsky, D., & Gibson, B. K. 2008, *MNRAS*, 390, 1133
 Binggeli, B. 1982, *A&A*, 107, 338
 Brainerd, T. G. 2005, *ApJ*, 628, L101
 Côté, P., Marzke, R. O., & West, M. J. 1998, *ApJ*, 501, 554
 Côté, P., et al. 2004, *ApJS*, 153, 223 (Paper I)
 Côté, P., et al. 2006, *ApJS*, 165, 57
 Côté, P., et al. 2007, *ApJ*, 671, 1456
 Faltenbacher, A., Li, C., White, S. D. M., Jing, Y.-P., Shu-DeMao, & Wang, J. 2009, *Research in Astronomy and Astrophysics*, 9, 41
 Ferrarese, L., et al. 2006, *ApJS*, 164, 334
 Ferrarese, L., Côté, P., Cuillandre, J.-C., et al. 2012, *ApJS*, 200, 4
 Hasegan, M., et al. 2005, *ApJ*, 627, 203
 Hashimoto, Y., Henry, J. P., & Boehringer, H. 2008, *MNRAS*, 390, 1562
 Jordán, A., et al. 2004a, *ApJS*, 154, 509 (Paper II)
 Jordán, A., et al. 2005, *ApJ*, 634, 1002 (Paper X)
 Jordán, A., et al. 2006, *ApJ*, 651, L25
 Jordán, A., et al. 2007, *ApJS*, 171, 101 (Paper XII)
 Jordán, A., et al. 2009, *ApJS*, 180, 54
 Larsen, S. S., Brodie, J. P., Huchra, J. P., Forbes, D. A., & Grillmair, C. J. 2001, *AJ*, 121, 2974
 Liu, C., Peng, E. W., Jordán, A., Ferrarese, L., Blakeslee, J. P., Côté, P., & Mei, S. 2011, *ApJ*, 728, 116
 McLaughlin, D. E., Harris, W. E., & Hanes, D. A. 1994, *ApJ*, 422, 486
 McLaughlin, D. E., Secker, J., Harris, W. E., & Geisler, D. 1995, *AJ*, 109, 1033
 Mei, S., et al. 2005, *ApJ*, 625, 121
 Mei, S., et al. 2007, *ApJ*, 655, 144
 Mieske, S., et al. 2006, *ApJ*, 653, 193 (Paper XIV)
 Moore, B., Diemand, J., Madau, P., Zemp, M., & Stadel, J. 2006, *MNRAS*, 368, 563
 Peng, E. W., et al. 2006a, *ApJ*, 639, 95
 Peng, E. W., et al. 2006b, *ApJ*, 639, 838
 Peng, E. W., et al. 2008, *ApJ*, 681, 197
 Peng, E. W., et al. 2011, *ApJ*, 730, 23
 Romanowsky, A. J., Strader, J., Brodie, J. P., et al. 2012, *ApJ*, 748, 29
 Searle, L., & Zinn, R. 1978, *ApJ*, 225, 357
 Strader, J., Romanowsky, A. J., Brodie, J. P., et al. 2011, *ApJS*, 197, 33
 Wang, Y., Yang, X., Mo, H. J., Li, C., van den Bosch, F. C., Fan, Z., & Chen, X. 2008, *MNRAS*, 385, 1511
 West, M. J. 1994, *MNRAS*, 268, 79
 West, M. J., & Blakeslee, J. P. 2000, *ApJ*, 543, L27
 Woodley, K. A. 2006, *AJ*, 132, 2424
 Yang, X., van den Bosch, F. C., Mo, H. J., Mao, S., Kang, X., Weinmann, S. M., Guo, Y., & Jing, Y. P. 2006, *MNRAS*, 369, 1293
 Yoon, S.-J., Yi, S. K., & Lee, Y.-W. 2006, *Science*, 311, 1129
 Yoon, S.-J., Lee, S.-Y., Blakeslee, J. P., et al. 2011, *ApJ*, 743, 150
 Zaritsky, D., Smith, R., Frenk, C., & White, S. D. M. 1997, *ApJ*, 478, 39